

1 **TITLE: Displacement of Water Molecules from**
2 **Receptor-Ligand Interface during Binding Interaction**

3 **Short Title: Desolvation of Receptor-Ligand Interface**

4 **AUTHOR: Ikechukwu Iloh Udema¹**

5 **Affiliation: ¹Department of Chemistry and Biochemistry, Research Division, Ude**
6 International Concepts Ltd., 862217, B. B. Agbor, Delta State, Nigeria.

7 **ORCID: <https://orcid.org/0000-0001-5662-4232>**

8 **Email address: udema_ikechukwu99@yahoo.com**

9
10
11
12
13
14
15
16
17
18
19
20
21
22
23
24
25
26
27
28
29
30
31
32
33
34
35
36
37
38
39
40
41
42
43
44
45
46
47
48
49

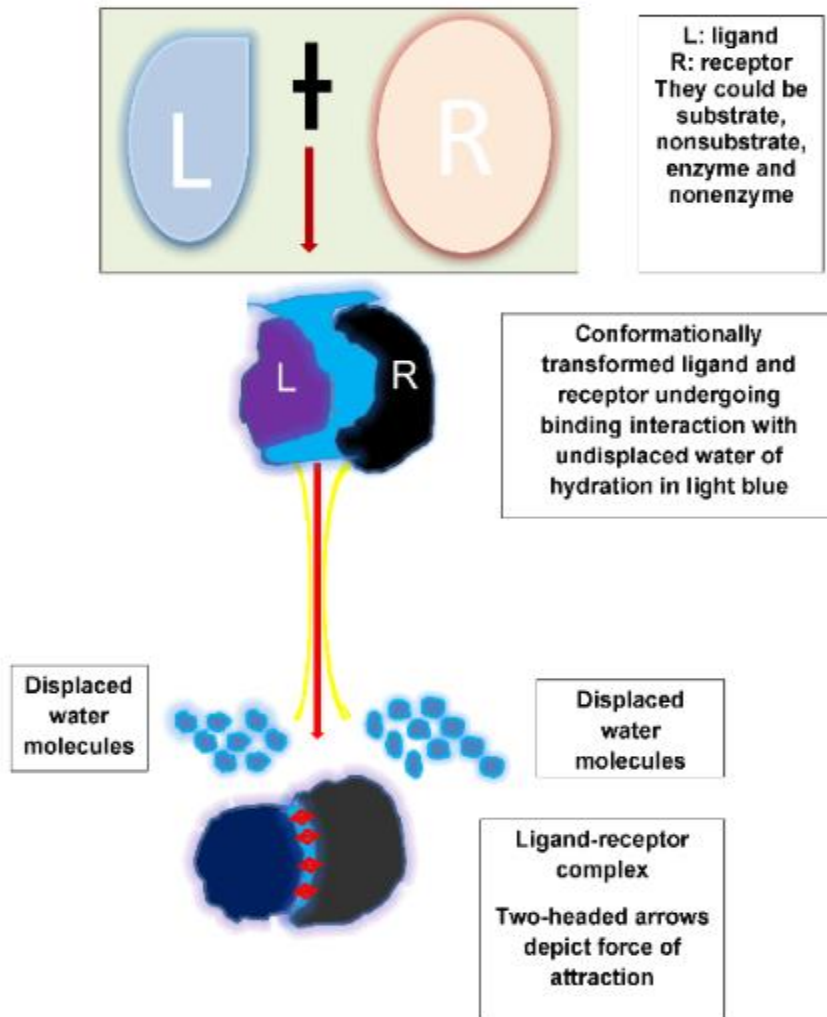
50 **ABSTRACT**

51 In almost all studies on the role of solvent in the binding of the ligand to a receptor, the focus had
52 always been on the thermodynamic stability of the complex formed. Hardly any attempt has been made to
53 quantify the number of solvent molecules released in the course of ligand (*e.g.*, substrate, pathogen,
54 drug, *etc.*) and receptor (enzymes, cell membrane, antibodies, *etc.*) binding interaction in recent times.
55 The goal of the study was to determine how to calculate the amount of solvent molecules displaced from
56 reactant species using nonequilibrium binding energy (NEBE), since desolvation is a prerequisite for the
57 development of a stable complex. Deriving relevant energy equations, such as the one for calculating the
58 number of molecules of desolvation, was one of the objectives. The methods are solely theoretical,
59 experimental (Bernfeld), and computational. According to the study's findings, the water of hydration
60 ranged from 338 to 400 water molecules, which corresponded to substrate (gelatinized potato starch)
61 concentrations between 5 and 10 g/L. The translational entropy gains, the corresponding thermodynamic
62 component, ranged from 91.4 to 133.1 J/mol K. The comparable values were 526.316 and 216.129 J/mol
63 K, respectively, at the highest hydrolysis velocity. In conclusion, the equation of NEBE can be explored
64 for the computation of water of desolvation in support of the observation that desolvation is part of the
65 driving forces that propel ligand-receptor binding. Further thermodynamic characterization of ligand-
66 receptor binding on the basis of desolvation needs to be done at different temperatures in the future.

67 **Keywords:** *Aspergillus oryzae*, Desolvation, Diffusivities, Nonequilibrium binding energy, Translational
68 entropy, Water

69 **PACS Number:** 87.15.A, 87.17.Jj.

GRAPHICAL ABSTRACT



70
71
72
73
74
75
76
77
78
79
80
81
82
83

1.0 INTRODUCTION

Over the years, researchers have swept through the discipline of soft matter physics, which aims to clarify how water molecules affect ligand-receptor interaction, binding, stability, *etc.*, in order to effectively create rational drugs. Rational medication design requires a precise treatment of the ligand-host protein interaction (Yoshida, 2017), which can be improved and directed by knowledge of nonequilibrium binding energy. A thorough grasp of the nonequilibrium binding energy involved in the formation of enzyme-substrate complexes may be useful in understanding other interactions, including those between drugs and proteins, antigens and antibodies, the dreaded SARS-CoV-2 and cell membrane. During the binding relationship between the enzyme and the substrate, which may also be desolvated, it is maintained that water must be displaced from the enzyme's binding sites. According to Szalai *et al.* (2024), the binding site water network plays a crucial role in ligand-protein binding, as evidenced by the notable changes in binding enthalpies between light and heavy water. Both the ligand and the protein are solvated before binding in a physiological setting, and at least a partial desolvation of both components occurs throughout the binding process (Szalai *et al.*, 2024; Zhang *et al.*, 2024). When it comes to desolvation and the substitution of ligand-protein and water-water interactions for ligand-water and protein-water interactions, the difference between apolar and polar moieties is essential. (Homans 2007, Ferenczy & Keserű 2012, Giordanetto *et al.*, 2019, Maurer & Oostenbrink, 2019).

The thermodynamic stability of the complex formed has always been the main focus of nearly all studies on the role of solvent in ligand-receptor binding. Years ago, the idea of the potential of mean free path, which is similar to Gibbs free energy in relation to complex formation, was of interest. At standard pressure and an appropriate temperature, the potential of mean force, PMF ($\Delta G(R_0)$), depends on the distance (R_0) between the two large molecules. The contributions to it come from the entropic ($-\Delta S(R_0)$) and enthalpic ($\Delta H(R_0)$) terms; the relative percentage of the two contributions depends on R_0 , and the stabilizing effects of the PMF's entropic and enthalpic contributions act in opposite directions to one another (Choudhury and Pettitt, 2006). This is why the concentration of the reactants (or ligand and receptor) is very relevant. In the logarithmic relationship between ΔG and binding affinity (K_d), a negative ΔG indicates stronger binding or, better yet, greater stability or spontaneity in binding. Water molecules influence enthalpy and entropy, impacting ΔG (Qu *et al.*, 2024). In a study years back, Michel *et al.* (2009) suggested how removal of water can increase the negative magnitude of the binding free energy change. Accounting for water's influence is crucial when calculating protein-ligand affinity (Zsidó & Hetényi, 2021). As per K_d , a dimensionless equilibrium constant had been proposed and used elsewhere (Udema & Onigbinde, 2019; Udema, 2025) since $\Delta G/RT$ is dimensionless and there is no basis for a standard state dissociation constant.

In light of the fact that water molecules interact with proteins and ligands during protein-ligand interaction, influencing entropy and enthalpy changes and, ultimately, ΔG (Chen & Wang, 2023), the question that remains is how many solvents (in this case, water) are likely to be released after the formation of an enzyme-substrate complex. As can be seen from the above, the main focus has been on the importance of the solvent in ligand-receptor binding. Almost no effort is made to measure the quantity of solvent molecules released during the binding contact between the ligand (substrate, pathogen, drug, *etc.*) and the receptor (enzymes, cell membrane, antibodies, *etc.*) in recent times. The goal of the work was to determine how to calculate the amount of solvent molecules displaced from reactant species using some aspects of bioenergetics principles, since desolvation is a prerequisite for the development of a stable complex. The objectives included figuring out how many molecules of desolvation—that is, how many water molecules are displaced from the receptor-ligand interface during binding interaction—and deriving the appropriate bioenergetics equations that allow them to be achieved.

2.0 BRIEF THEORY

Previously, the motion of dissolved and hydrated particles was described as those that do work over the length of a displacement against viscosity and, in some cases, against opposing attractive or repulsive forces (Udema, 2017). In this brief theory, care is taken to avoid confusing potential and kinetic energies viewed against the backdrop of a scenario of conservative field forces (Udema, 2020). There are two types of forces, namely short- and long-range forces; the latter come into cumulative effect after the long-range forces have narrowed the intermolecular distance. This explains why nonpolar (or hydrophobic) molecules, whether they exist as a homogeneous substance or in combination with other polar substances, have a high melting point. In these situations, bulk and steric factors are not precluded. Moving forward, two equations (Udema, 2017) are herein stated as follows:

139
$$u_i = 4\pi\alpha_E\dot{R}(R_0 - \dot{R})D_EC_{ES}, \quad (1)$$

140 The equation specifies the translational velocity (u_i) of any solute in solution up to a target solute where
 141 the interparticle distance (\dot{R}) is the sum of two radii, namely, the hydrodynamic radii of the substrate, S (or
 142 ligand, L), and of the enzyme, E (or receptor, R), designated respectively as R_S (R_L) and R_E (R_R) if there
 143 are no perturbative attractive or repulsive forces. In this case the only force originates from the thermal
 144 energy of bulk solution. D_E , C_{ES} , and R_0 (to be defined shortly) are the translational diffusion coefficient of
 145 E or R if mobile, the molar concentration of ES or RL, representing respectively, the enzyme-substrate
 146 complex and receptor-ligand complex if all are mobile, and α_E and α_S are given as:

147
$$\alpha_E = \left(\frac{M_3}{M_2}\right)^{1/2} / [(M_3/M_2)^{1/2} + 1] \quad (2a)$$

148
$$\alpha_S = \left(\frac{M_2}{M_3}\right)^{1/2} / [(M_2/M_3)^{1/2} + 1] \quad (2b)$$

149 The alternatives are respectively, $\alpha_E = 1 - \alpha_S$ and $\alpha_S = 1 - \alpha_E$; each represents a fraction of the total
 150 distance covered while advancing towards each other (the enzyme, E, and substrate, S); the lower molar
 151 mass solute having a higher fraction than the higher molar mass solute. Of course, this study deals with
 152 not less than two species that are mobile in solution. The second equation is:

153
$$u_i = 4\pi\alpha\dot{R}(R_0 - \dot{R})D_S C_{ES}, \quad (3)$$

154 where the subscript S refers to the substrate (ligand). Henceforth, the enzyme and substrate will be
 155 adopted, and therefore, they may be generalizable to receptors and ligands. If up to a point electrostatic
 156 forces come into effect, the intermolecular distance (R_0) where such forces commence needs to be
 157 determined. As stated earlier, this section needs to be brief as further details can be found in the literature
 158 (Udema, 2017). The intermolecular distance where attractive or repulsive electrostatic forces commence
 159 is given as:

160
$$R_0 = \frac{\dot{R}}{1 - S_{i-1}/S_{i-2}^2} \quad (4)$$

161 where S_{i-1} is the slope from the plot of the square of the frequency ($\dot{\nu}$) of collision between E (or R) and S
 162 (or L) versus $1/[R_{int}(R_{int} - \dot{R})]$. R_{int} is the average intermolecular distance.

163 Meanwhile, for any two solutes in solution advancing towards each other regardless of any
 164 obstacles, if both solutes can be influenced mutually by electrostatic forces (attraction in this case), then
 165 there should be two forms of kinetic energy, one of thermal origin and the other of electrostatic origin;
 166 hence, Eq. (4) specifies the intermolecular distance at which mutual attractive forces commence. Thus,
 167 Newtonian mechanics comes into relevance such that $mu_2^2 = mu_0^2 + 2F\Delta x$ (m , u_0 , u_2 , F , and Δx are the
 168 mass of solute, initial thermally driven velocity, final or peak velocity, force, and distance covered
 169 following attractive electrostatic interaction). The electrostatic component creating directionality akin to
 170 electrostatic steering (Wade et al., 1998), earlier shown in the literature (Udema, 2017), is derived in a
 171 simpler manner as follows:

172
$$\phi = 13.8564(\alpha\pi^3\eta R_E P)^{1/2} \epsilon_r \epsilon_0 [R_{int}^3 (R_{int} - \dot{R})] / e^2 \quad (5)$$

173
$$\dot{\nu} = 0.288675 \left(\frac{P}{\alpha\pi\eta R_E R_{int} (R_{int} - \dot{R})} \right)^{1/2} \quad (6)$$

174 where $\dot{\nu}$ is the frequency of collision given by Smoluchowski's equation between the enzyme (the bullet
 175 molecule) and the larger molecule, the polysaccharide. The enzyme and the substrate, regardless of size,
 176 remain the receptor and ligand, respectively. Smolucowski's equation is $2\pi\dot{R}D_EC_{ES}$. Solving for the square
 177 root of P gives:

178
$$P^{1/2} = \frac{\dot{\nu}[\alpha\pi\eta R_E R_{int} (R_{int} - \dot{R})]^{1/2}}{0.288675} \quad (7)$$

179 Substitute Eq. (7) into Eq. (5) to give:

180
$$\phi = \frac{\dot{\nu}[13.8564\alpha\pi\eta R_E R_{int}^2 (R_{int} - \dot{R})\pi\epsilon_r\epsilon_0]}{0.288675 e^2} \quad (8)$$

181 Meanwhile, Eqs (5) through (8) are regarded as general equations in that, though R_{int} represents average
 182 intermolecular distance, all equations can have R_{int} replaced by the intermolecular distance (R_0) where
 183 electrostatic attraction commences. The physical meaning of ϕ stems from the fact that there are a
 184 significant number of cases in which a mixture of solutes comprises small polar, small and large ionic
 185 compounds; in all, there could be polar-polar, polar-hydrophobic, ionic-ionic, ionic-polar, and ionic-
 186 hydrophobic interactions. Each of them has a descriptive equation, but it is not certain what the net
 187 charge of macromolecules like proteins and dipole moment of the polar molecules may be; van der Waals

188 force may not easily be quantifiable on a case-by-case basis. Considering the fact that there are long-
 189 and short-range attractive forces, without information about the net charges and dipole moment, these
 190 forces that generate kinetic energy of motion rather than the potential energies (being conventionally
 191 negative as the lower values but zero at the highest value by virtue of position relative to another position
 192 in space) are summed up to give:

$$193 \quad 2K.E. = \frac{\phi e^2}{4\pi\epsilon_r\epsilon_0 R} \quad (9)$$

194 The sum of all long— and short—range attractive forces, including hydrophobic interactions, may be ϕ —
 195 fold greater or less than $e^2/4\pi\epsilon_r\epsilon_0$; if $\phi > 1$, it may be greater; if $\phi < 1$ (a fraction), it may be less. If there
 196 are binding interaction between particles with a unit formal charge and weakly polar charge particles, $\phi <$
 197 1; the converse is case if the formal charge is greater than one. The following equations are not meant to
 198 be derived but are used to show the difficulty of understanding information about unknown, independent
 199 variables, like dipole moments; therefore, they are labeled with separate Roman numbers and used in a
 200 qualitative analysis.

$$201 \quad \beta\omega(R) \approx -\xi_{ii} - \xi_{i-in} - \xi_{in} - \xi_{id} - \xi_{dd} \quad (9i)$$

202 where $(-\xi_{ii})$, $(-\xi_{i-in})$, $(-\xi_{in})$, $(-\xi_{id})$, $(-\xi_{dd})$, β , and $\omega(R)$ are the potential energy of interaction (I_E)
 203 between two ionic molecules, ion-induced I_E , induced dipole-dipole (van der Waal's kind) I_E , ion-dipole I_E ,
 204 dipole-dipole I_E , $1/k_B T$ (where k_B and T are the Boltzmann constant and thermodynamic temperature
 205 respectively), and PMF respectively. As an example of one of those equations is the equation of dipole-
 206 dipole I_E given as (Lund, 2006):

$$207 \quad \text{Dipole-dipole interaction energy} = -k_B T \frac{(I_B \mu_A \mu_B)^2}{3R^6} \quad (9ii)$$

208 where R , I_B , and μ are the distance between interacting particles, Bjerrum length, electric dipole moment
 209 respectively. For strongly ionized protein—polysaccharide I_E with a net charge in the protein while the
 210 polysaccharide is polar, in a given buffer, the $\omega(R)$ (Udema, 2017) is given as:

$$211 \quad V_{2-3S} = \frac{-(I_B Z_2 \mu_S)^2 (e^{-\kappa(R-a)})^2}{6R^4 (1+\kappa a)^2} \quad (9iii)$$

212 κ and a are the inverse Debye screening length and the closest distance between the “central ion”
 213 (protein b or any other charged substrate such as phosphate containing starch) and surrounding ions
 214 which is approximately the protein radius respectively. The overall kinetic energy, a summation of long
 215 range and all available short range energies is given as:

$$216 \quad \frac{\phi e^2}{8\pi\epsilon_r\epsilon_0} = -\beta\omega(R)/2 \quad (9iv)$$

217 To some degree of specifics, one may have:

$$218 \quad \frac{\phi e^2}{8\pi\epsilon_r\epsilon_0} = -k_B T \frac{(I_B \mu_A \mu_B)^2}{3R^6} - \frac{(I_B Z_2 \mu_S)^2 (e^{-\kappa(R-a)})^2}{6R^4 (1+\kappa a)^2} - \dots \quad (10)$$

219 Given that achieving near-accuracy in all measurements is a daunting task, the first part of the qualitative
 220 analysis involves figuring out how to locate all independent variables and, maybe, every type of
 221 operational I_E by exploring very complex instrumentation. Structural analysis of the large molecules and
 222 the complex formed are not avoidable. A way out is the formulation of a sort of quasi-Coulomb equation
 223 on account of which the factor phi, ϕ , has to be substituted into Eq. (10). Next substitute Eq. (8) in which
 224 R_{int} is substituted for R_0 into Eq. (9) to give:

$$225 \quad \xi_{El} = \frac{\dot{v}[12\pi\eta R_E R_0^2 (R_0 - \dot{R})]}{\dot{R}} \quad (11)$$

226 The total energy (ξ_T), combining thermal and electrostatic energies for the two particles moving towards
 227 each other, is given as:

$$228 \quad \xi_{TL} = 6\pi\eta R_E * 4\pi\gamma_E \dot{R} (R_0 - \dot{R})^2 D_E C_{ES} + 6\pi\eta R_S * 4\pi\gamma_S \dot{R} (R_0 - \dot{R})^2 D_S C_{ES} + \frac{\dot{v}[24\gamma_E \pi \eta R_E R_0^2 (R_0 - \dot{R})]}{2\dot{R}} + \frac{\dot{v}[24\gamma_S \pi \eta R_S R_0^2 (R_0 - \dot{R})]}{2\dot{R}} \\ 229 \quad = 24\pi\eta \left[R_E \gamma_E \left(\pi \dot{R} (R_0 - \dot{R})^2 D_E C_{ES} + \frac{R_0^2 (R_0 - \dot{R}) \dot{v}}{2\dot{R}} \right) + R_S \gamma_S \left(\pi \dot{R} (R_0 - \dot{R})^2 D_S C_{ES} + \frac{R_0^2 (R_0 - \dot{R}) \dot{v}}{2\dot{R}} \right) \right] \quad (12)$$

230 Note that the substitution of Eqs (1) and (2) separately into $6\pi\eta R_E$ and $6\pi\eta R_S$ respectively and multiplying
 231 respectively by $\gamma_E (R_0 - \dot{R})$ and $\gamma_S (R_0 - \dot{R})$ give the work down against the resistance of the medium.
 232 Meanwhile, ξ_T is equal to the sum of all thermal energies (ξ_{ST}) driving the motion of the solution
 233 components, including some (if not all) of the departing water of hydration. Going forward, the reader is
 234 reminded that the effective energy (ξ_{eff}) of motion in a given liquid solvent or mixture in a liquid state,
 235 under the influence of thermal energy, is given as (Udema, 2016):

$$\xi_{eff} = \left[m_i \left(\frac{6k_B T D_i}{L} \right)^2 \right]^{1/3} \quad (13)$$

where, L , k_B , T , m_i and D_i are respectively, the cube root of the molar volume of the solvent (water), Boltzmann constant, thermodynamic temperature, mass of any solution component, and translational diffusion coefficient of solution components. Expectedly high-ranking scholars, notably in advanced scientific communities in the Americas, Europe, and Asia, etc., may raise objections, but it is inconceivable that biological fluid components, such as water, can possess thermal energy equal to $3 k_B T$ as to imply “a reverse unguided evolution” akin to “an American and in particular Indian action movie in which the lead actor disappears into the thin air from the roof of a high-rise building; of course, the movie producers advise the young ones against any attempt to replicate such action.”

$$\xi_{ST} = \left[m_S \left(\frac{6k_B T D_S}{L} \right)^2 \right]^{1/3} + \left[m_E \left(\frac{6k_B T D_E}{L} \right)^2 \right]^{1/3} + \Phi_d \left[m_W \left(\frac{6k_B T D_W}{L} \right)^2 \right]^{1/3} \quad (14)$$

where m_W and ‘ Φ_d ’ are respectively, the mass of one molecule of water and number of water molecules released per enzyme-substrate (ES) complex formation.

$$\xi_{ST} = \left(\frac{36k_B^2 T^2}{L^2} \right)^{1/3} \left(D_S^{2/3} m_S^{1/3} + D_E^{2/3} m_E^{1/3} + \Phi_d D_W^{2/3} m_W^{1/3} \right) \quad (15)$$

Given that $\xi_{ST} = \xi_{\pi}$ (Eq. (12)), then, for the purpose of simplicity, consider the following:

$$\begin{aligned} \bar{e} &= R_E \gamma_E \left(\pi \dot{R} (R_0 - \dot{R})^2 D_E C_{ES} + \frac{R_0^2 (R_0 - \dot{R}) \dot{v}}{2 \dot{R}} \right) \\ \hat{s} &= R_S \gamma_S \left(\pi \dot{R} (R_0 - \dot{R})^2 D_S C_{ES} + \frac{R_0^2 (R_0 - \dot{R}) \dot{v}}{2 \dot{R}} \right) \\ \Phi_d &= \frac{1}{D_W^{2/3} m_W^{1/3}} \left[24 \pi \eta \left(\frac{L^2}{36 k_B^2 T^2} \right)^{1/3} (\bar{e} + \hat{s}) - (D_S^{2/3} m_S^{1/3} + D_E^{2/3} m_E^{1/3}) \right] \end{aligned} \quad (16)$$

3.0 MATERIALS AND METHODS

3.1 Equipment

An electronic weighing machine was purchased from Wensler Weighing Scale Limited, and a 721/722 visible spectrophotometer was purchased from Spectrum Instruments, China. A hand pH meter was purchased from Hanna Instruments, Italy.

3.2 Chemicals and their preparation

As explored in earlier studies (Udema, 2023), *Aspergillus oryzae* alpha-amylase (EC 3.2.1.1) and insoluble potato starch, whose molar mass is ~ 64540 kg/mol. (Tomasik, 2009) were purchased from Sigma-Aldrich, USA. Tris HCL, 3, 5-dinitrosalicylic acid, maltose, and sodium potassium tartrate tetrahydrate were purchased from Kem Light Laboratories in Mumbai, India. Hydrochloric acid, sodium hydroxide, and sodium chloride were purchased from BDH Chemical Ltd., Poole, England. Distilled water was purchased from the local market. The molar mass of the enzyme is 52 k Da (Sugahara et al., 2013). A gelatinized insoluble potato starch whose concentration is equal to 1 g/100 mL was subjected to serial dilution give concentrations ranging between 5 and 10 g/L for the assay in which $[S_0] \gg [E_0]$ (0.0005 g/L). A concentration of *A. oryzae* alpha-amylase equal to 0.0005 g/L was prepared in a Tris HCl buffer solution at a pH of 7.0.

3.3 Method

The enzyme was assayed using gelatinized potato starch in accordance with Bernfeld's (3, 5-dinitrosalicylic acid) technique (Bernfeld, 1955). Using maltose as a standard, the amount of reducing sugar generated after the substrate hydrolyzed in three minutes was measured at 540 nm, with an extinction coefficient of 181 L/mol.cm. The assay was carried out at 25°C. The maximum intermolecular distance (R_{int}) was determined using the equation: $R_{int} = (V/(n_S + n_E) N_A)^{1/3}$ where n_E , n_S , V , and N_A are number of moles of the enzyme and substrate, volume of the reaction mixture, and Avogadro's number respectively. The minimum intermolecular distance wherein mutual electrostatic perturbation commences is determined as described elsewhere (Udema, 2017). The diffusion coefficient of the starch was computed using the equation for large molar mass polymers given as $D_2 = D_1 (M_1/M_2)^{1/3}$ where $M_2 > M_1$; the latter represent different molar masses while the D_s are different diffusivities ($D_1 > D_2$). The hydrodynamic radius of the starch computed using Stokes-Einstein equation is that of a sphere whose volume is equal to that of a nonspherical starch polymer. The diffusivity of water at 298.15 K used was $2.3 \exp. (-11) \text{ m}^2/\text{s}$ (Camposano et al., 2025). That of *A. oryzae* was computed using an arbitrarily chosen radius of 2.51 nm substituted into Stokes-Einstein equation.

3.4 Statistics

285 The mean catalytic velocity of hydrolysis of gelatinized starch was calculated using a Casio
 286 scientific calculator (fx-991MS-China). Gaussian statistics are not appropriate. Thus, the best method for
 287 determining the variance (σ^2) and, in turn, the standard deviation for a population (n) of size three is to
 288 use a nonparametric statistical approach (Hozo et al., 2005). Results are presented as mean \pm SEM.
 289 Hozo et al. (2005) equation is:

$$\sigma^2 = \frac{(n+1)[(n^2+3)(a-2m+b)^2+4n^2(b-a)^2]}{48n(n-1)^2} \quad (18)$$

291 where n , a , b , and m are the size of the sample (data points, 3 in this research), the smallest value, the
 292 largest value, and the median respectively. Microsoft Excel (2010) was used to carry out graphical plots.

293 4. RESULTS AND DISCUSSION

294 4.1 Results

295 Moving forward, the number of molecules of the enzyme-substrate (ES) complex is computed as shown
 296 in Table 1. Such parameter is used for the computation of the frequency of collision between the enzyme
 297 and the substrate using Smolucowski's equation. The frequency is needed for the graphical determination
 298 of the first and second slopes stated in Eq. (4).

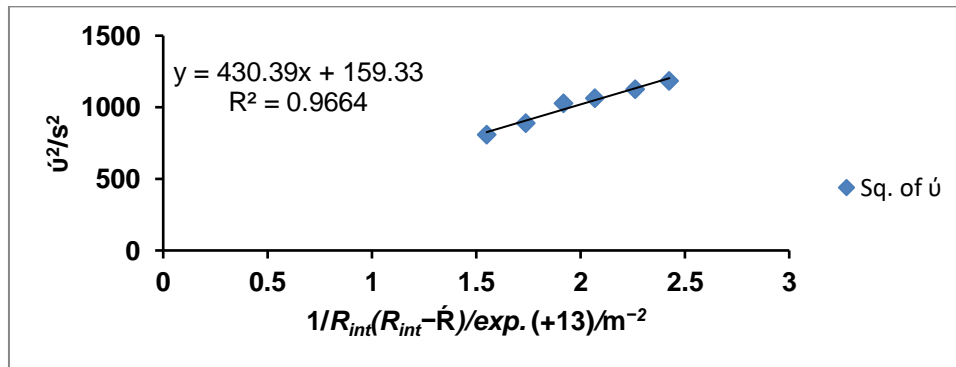
299 **Table 1: The velocities (v) of hydrolysis of gelatinized starch and the number (N_{ES}) of molecules
 300 ES complex**

301 [S ₀]/g/l	v /exp. (-5) /mol./l/min	N_{ES} / exp. (+18)
303 5	6.493 \pm 0.118	3.72 \pm 0.035
304 6	6.852 \pm 0.052	3.90 \pm 0.023
305 7	7.324 \pm 0.106	4.12 \pm 0.023
306 8	7.452 \pm 0.091	4.27 \pm 0.023
307 9	7.657 \pm 0.175	4.39 \pm 0.021
308 10	7.847 \pm 0.101	4.50 \pm 0.018

309 Molar concentrations were adopted for computational convenience.

310 The computed R_{int} values are used for the computation of the minimum intermolecular distance, R_0 and the
 311 differences between them and the sum of the hydrodynamic radii of the substrate and enzyme as shown in Table 2;
 312 the computation of R_0 , requires that the slopes indicated in Eq. (4) have to be graphically determined. The first slope
 313 is derived from Fig. (1).

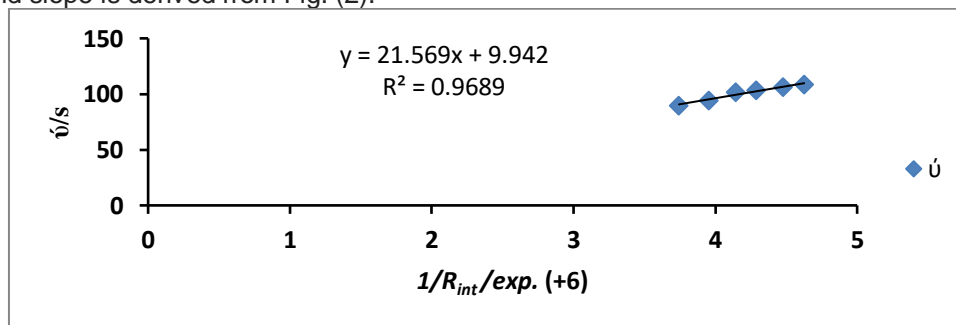
314



315

316 **Figure (1): Determination of the first slope $S_{L1} = 430.39 \text{ exp. } (-13) \text{ m}^2/\text{s}^2$**

317 The second slope is derived from Fig. (2).



318

319 **Figure (2): Determination of the second slope $S_{L2} = 21.569 \text{ exp. } (-6) \text{ m/s}$**

320 **Table 2: Intermolecular distance (R_{int}) and difference between R_{int} and sum of hydrodynamic radii**
 321 **(\bar{R}) of two different molecules**

322	$R_{int}/exp. (-7)/m$	2.671	2.530	2.414	2.331	2.233	2.161
323	$(R_{int}-\bar{R})/exp. (-7)/m$	2.416	2.275	2.159	2.073	1.979	1.906

324 The first slope (S_{t1}) for the computation of intermolecular distance (R_0) where longer range electrostatic attraction
 325 began is obtained from the plot of \dot{u}^2 versus $1/R_{int}$ ($R_{int}-\bar{R}$); the second slope (S_{t2}) is obtained from the plot of \dot{u} versus
 326 $1/R_{int}$. (Udema, 2017) Eq. (4) is fitted to the two slopes for the computation of R_0 (40.436 nm); $R_0-\bar{R} = 3.74089$ nm; \bar{R}
 327 $= R_E + R_S = 36.6953$ nm; $R_S = 34.18532358$ nm

328 All the relevant values in Tables 1 and 2 were deployed and substituted into the relevant
 329 equations in the theoretical section to give for the first time, number of water of desolvation. Expectedly,
 330 the number of water of desolvation showed increasing trend with increasing substrate concentration
 331 (Table 3). The cognate entropy changes, which also showed a similar trend, were computed based on the
 332 premise that there is an increase in the number of free solvent molecules in the bulk following
 333 desolvation, which translates into an increase in entropy in a reaction volume of one cubic meter. The
 334 values of the water of desolvation, Φ_d per ES, ranged between approximately 338 and 400, while the
 335 total, $\Phi_d * N_{ES}$, ranged between 1.3 and 1.85 *exp. (+21)*; the cognate entropic energy, the translational
 336 entropy change, ranged between 91.4 and 133.1 J/mol K. As stated in the footnote of Table 3, the
 337 maximum amount of water of desolvation and, hence, the entropic term were calculated based on the
 338 idea that the water of desolvation can be thought of as a product in a reaction mixture that complies with
 339 Michaelian kinetics. At saturation level ($[ES]=[E_0]$), the maximum Φ_d , $\Phi_d * N_{ES}$, and $T\Delta S_{trans}$ values were
 340 526.316, 3.048 *exp. (+21)*, and 216.129 J/mol. K, respectively.

341 **Table 3: Number (Φ_d) of water molecules per ES, total displaced and translational**
 342 **entropy (ΔS_{trans}) gain of displaced water molecules**

343						
344	$[S_0]/g/L$	5	6	7	8	9
345	Φ_d	337.68	358.34	382.28	391.66	391.66
346	$\Phi_d * N_{ES}$	1.256	1.398	1.606	1.672	1.755
347	<i>(exp. (+21))</i>					
348	$T\Delta S_{trans}$	91.37	101.45	116.20	120.92	126.75
349	<i>(J/mol. K)</i>					

350
 351 Maximum Φ_d , $\Phi_d * N_{ES}$, and $T\Delta S_{trans}$ values at saturation level ($[ES]=[E_0]$) were 526.316, 3.048 *exp. (+21)*, and
 352 216.129 J/mol. K respectively. The translational entropy of the departing water molecules in the course of desolvation
 353 is computed on the premise that there is an increase in the number of free solvent molecules in the bulk, which
 354 translates into an increase in entropy in a reaction volume of one cubic meter. Thus, entropic energy is given as:

355
$$T\Delta S_{trans} = RT \ln \frac{18(\Phi_d N_{ES} + N_A/18)}{N_A}$$
 where R is the universal gas constant.

356 4.2 Discussion

357 This discussion serves to relate water of desolvation and translational entropy in this study to
 358 literature concern for the binding process enhanced by desolvation. The argument that the decrease in
 359 water-accessible surface area upon folding leads to a significant increase in water's translational entropy,
 360 overcoming the loss of protein's conformational entropy (Harano & kinoshita, 2005), may also explain the
 361 driving force behind ligand-receptor (LR which could be ES) complex formation. The entropic gain, driven
 362 by water molecules' freedom of movement, may be a key factor in stabilizing the folded protein structure
 363 besides the impact of hydrogen bond networks. This suggestion, however, is of hypothetical significance.
 364 Nonetheless it may be relevant in the stability of LR. Examples of concern for the release of water in the
 365 course of binding had been for decades as stated earlier. Thus, there is the case of hinge motions
 366 involving the ATP lid domain and the nucleoside monophosphate binding domain closing over their
 367 respective substrates, in which water is excluded from the enzyme's active site during the phosphoryl
 368 transfer reaction (Vonrhein et al., 1995, Muller et al., 1996). In other scenarios the source of an entropy
 369 increase following the binding of a ligand to a receptor, is the release of the water molecules from the
 370 binding pocket and from around the ligand to get more freedom in the bulk phase, purported to be
 371 investigated with unspecified, newly developed method (Ahmad et al., 2017).

372 It is equally expedient to realize that desolvation is not total, particularly with respect to the
373 enzyme, which requires conserved water for catalysis and stability. This notwithstanding, there are inner
374 and outer hydration layers in which there are grades of water densities; some have greater electrostriction
375 than the others. The idea that "prior to binding, the ligand-free binding pocket is occupied by water
376 molecules characterized by a paucity of H-bonds and high mobility resulting in an imperfect hydration of
377 the critical residue Asp189" (Scheibel et al., 2018) of the enzyme supports the problem of loosely bound
378 water molecules, which are likely to easily undergo desolvation. For instance, crucial residue Asp189 of
379 the lipase active site is not fully hydrated because water molecules with a high degree of mobility (loosely
380 bound water molecules) and few H-bonds occupy the ligand-free binding pocket before binding. This
381 phenomenon can enhance the elucidation of how water affects protein–ligand recognition and is probably
382 a major factor driving ligand binding via water displacement (Scheibel et al., 2018). Further to this, is the
383 observed decrease in protein dynamics consistent with the measured decrease in the intrinsic
384 volume, V_M (1.4–2.1%), of RNase A upon the binding to 2'-CMP or 3'-CMP (Dubins et al., 2000). This
385 information, applicable to any other enzyme-substrate binding reaction, such as the one with gelatinized
386 starch and amylase in this study, suggests that the binding of 2'-CMP or 3'-CMP to RNase A releases
387 between 210 ± 40 water molecules to the bulk state (Dubins et al., 2000). This value (210), though not
388 within the range of 338 to 400 (Table 3) reported in this study for amylase, is nevertheless good evidence
389 that the model developed in this study could be valid.

390 The reaction rate can change in response to the amount of water content in a reaction mixture.
391 Desolvation is likely a type of enzyme or substrate dependence that varies among different enzymes.
392 Studies on *Candida rugosa* lipase using different liquids as medium of reaction, showed that the highest
393 reaction rate was obtained in n-hexane and the ionic liquid [BMIM]PF₆ when the concentrations of water
394 were 0.15 mol/dm³ and 0.38 mol/dm³, respectively. In the more polar tetrahydrofuran, [BMIM]BF₄ esters
395 were produced at a very low reaction rate which was observed to be only slightly dependent on the
396 concentration of water (Lajtai-Szabó et al., 2020). The number of water molecules released could
397 dependent on the composition of reaction medium, pH, temperature, ionic strength, nature of the
398 substrate and enzyme. Furthermore, a high concentration of the enzyme or substrate results in high
399 viscosity, low water potential, and reduced translational velocities, which reduce the likelihood that there
400 are enough water molecules in the outer hydration layer to be displaced and, in turn, lower the velocity of
401 product formation.

402 The solvation free energy change is attributed to the solvation structure change due to the ligand
403 binding by the host protein (Yoshida, 2017). The solvation structure is changed when the ligand binds to
404 its recognition site because the hydrogen bonds are broken, rearranging the hydrogen bond network in
405 the solvent water. Understanding the thermodynamic process of molecule recognition is essential since
406 this change in solvation also modifies the solvent's entropy (Yoshida, 2017). In particular, it has been
407 proposed that the expulsion of thermodynamically unfavorable water molecules during complex formation
408 enhances the ligand's affinity (Young et al., 2007, Abel et al., 2011). This may be in line with the finding in
409 this study that the translational entropy gain ranging between 91.4 and 133.1 J/mol K of the departing
410 water molecules (desolvation) enhances and stabilizes the complex. Additionally, it should be noted that
411 not only the protein but also the ligand itself needs to be, at least partially, desolvated and thereby
412 influence binding. Research has shown that hydrogen bonds can enhance binding when both the donor
413 and acceptor have significantly stronger or weaker hydrogen bonding capabilities than water, while mixed
414 strong-weak pairings can decrease affinity due to interference with bulk water (Chen et al., 2016).

415 Based on all related issues in the literature, one can state in summary that water displacement
416 typically contributes to favorable entropy ($T\Delta S > 0$) and enthalpy ($\Delta H < 0$) changes, which, when combined
417 with hydrogen bonding changes that affect ΔH either positively or negatively, will ultimately affect the
418 overall ΔG (Zhang et al., 2024); if stronger hydrogen bonds are formed between the protein and ligand,
419 ΔH decreases, stabilizing the complex; however, if hydrogen bonds are broken without equivalent
420 replacements, the enthalpy may increase, making the binding less favorable (Chen et al., 2016). Thus, it
421 appears that low water potential bulk concentration and insufficient solvent desolvation may inhibit the
422 formation of the LR complex. A minimum water potential is necessary for the complex's functional groups
423 and the loose outer hydration layer to form a network of hydrogen bonds, as well as for translational
424 motion that can bring the enzyme and substrate close together.

425 **CONCLUSION**

426 The derived equations could be deployed for the computation of the water of desolvation
427 following ligand-receptor binding, exemplified by the results from this study, which showed a range of 338

428 to 400 water molecules with a corresponding thermodynamic component, translational entropy gain
429 ranging between 91.4 and 133.1 J/mol K. Further thermodynamic characterization of ligand-receptor
430 binding on the basis of desolvation needs to be done at different temperatures in the future. That will
431 entail the use of nonequilibrium binding energy to generate a number of waters of desolvation at different
432 temperatures, which, as long as such water molecules are regarded as byproducts, could be fitted to the
433 Michaelian equation, as was done in this research.

434 **DISCLAIMER (ARTIFICIAL INTELLIGENCE)**

435 Author(s) hereby declare that NO generative AI technologies such as Large Language Models
436 (ChatGPT, COPILOT, etc.) and text-to-image generators have been used during the writing or editing of
437 this manuscript.

438 **DEDICATION**

439 Dr. (Honoris Causa) Samuel Osaigbovo Ogbomudia (Brigadier General) was one-time military
440 governor of the defunct Mid-West State of Nigeria and in the latter years became an active politician.
441 Among many selfless accomplishments, only one is intentionally mentioned. This is the establishment of
442 the state transport company. The vehicles were not customized after his name; rather, they were given
443 the inscription "Mid-West Line," which greatly influenced private investors within and out of the state to
444 establish transport companies in which their vehicles bore the inscription, the name, and then "Line," e.g.,
445 "Ekenedilichukwu Line." The state transport company was efficient and profitable. To him, I dedicate this
446 study for his selfless service to humanity..

447 **ACKNOWLEDGEMENT**

448 I am very grateful to my siblings for their financial and in-kind support. Grammar-
449 checking services by QuillBot Company are also appreciated.

450 **AUTHORS' CONTRIBUTIONS**

451 The sole author designed, analyzed, interpreted and prepared the manuscript.

452 **CONSENT**

453 NA

454 **ETHICAL APPROVAL (WHERE EVER APPLICABLE)**

455 NA

456 **REFERENCES**

- 457 Abel, R., Salam, N. K., Shelley, J., Farid, R., Friesner, R. A., & Sherman, W. (2011). Contribution of
458 explicit solvent effects to the binding affinity of small-molecule inhibitors in blood coagulation factor serine
459 proteases. *ChemMedChem*, 6(6), 1049–1066. <https://doi.org/10.1002/cmdc.201000533>
- 460 Ahmad, M., Kalinina, O. & Lengauer, T. Entropy gain due to water release upon ligand binding. *Journal of*
461 *Cheminformatics* 6 (Suppl 1), P35 (2014). <https://doi.org/10.1186/1758-2946-6-S1-P35>
- 462 Bernfeld, P (1955) Amylases, alpha and beta, *Methods. Enzymol.* 1, 149–152.
463 [https://doi.org/10.1016/0076-6879\(55\)01021-5](https://doi.org/10.1016/0076-6879(55)01021-5)
- 464 Camposano, A. V. C., Nordhagen, E. M., Sveinsson, H. A., & Malthe-So Renssen, A. (2025). Genetic
465 Algorithm Workflow for Parameterization of a Water Model Using the Vashishta Force Field. *The Journal*
466 *of Physical Chemistry. B*, 129(4), 1331–1342. <https://doi.org/10.1021/acs.jpcc.4c06389>
- 467 Dubins, D. N., Filfil, R., Macgregor, R. B., Chalikian, T. V. (2000). Role of Water in Protein–Ligand
468 Interactions: Volumetric Characterization of the Binding of 2'-CMP and 3'-CMP to Ribonuclease A *The*
469 *Journal of Physical Chemistry B* 2000, 104(2), 390–401, <https://doi.org/10.1021/jp992138d>
- 470 Harano, Y., & Kinoshita, M. (2005). Translational-entropy gain of solvent upon protein folding. *Biophysical*
471 *journal*, 89(4), 2701–2710. <https://doi.org/10.1529/biophysj.104.057604>
- 472 Hozo, S. P., Djulbegovic, B., & Hozo I. (2005) Estimating the means and variance from the median range
473 and the size of a sample. *BMC Medical Research Methodology.* 5(13),1-10.
474 <https://doi.org/10.1186/1471-2288-5-13>
- 475 Lajtai-Szabó, P., Nemestóthy, N., and Gubicza, L. (2020). The role of water activity in terms of enzyme
476 activity and enantioselectivity during enzymatic esterification in nonconventional media *Hungarian Journal*
477 *of Industry and Chemistry* 48(2), 9–12 <https://doi.org/10.33927/hjic-2020-22>
- 478 Lund, M. (2006) Electrostatic interactions in and between biomolecules Lund University Ph.D. *Thesis*
- 479 Michel, J., Tirado-Rives, J., & Jorgensen, W. L. (2009). Energetics of displacing water molecules from
480 protein binding sites: consequences for ligand optimization. *Journal of the American Chemical*
481 *Society*, 131(42), 15403–15411. <https://doi.org/10.1021/ja906058w>

482 Müller, C. W., Schlauderer, G. J., Reinstein, J., & Schulz, G. E. (1996). Adenylate kinase motions during
483 catalysis: An energetic counterweight balancing substrate binding. *Structure (London, England:*
484 1993), 4(2), 147–156. [https://doi.org/10.1016/s0969-2126\(96\)00018-4](https://doi.org/10.1016/s0969-2126(96)00018-4)

485 Neurath, H. & Cooper, G. R. (1940). The diffusion constant of tomato bushy stunt virus, *Journal of*
486 *Biological Chemistry*, 135 (2), 455-462, [https://doi.org/10.1016/S0021-9258\(18\)73114-1](https://doi.org/10.1016/S0021-9258(18)73114-1)

487 Qu, X., Dong, L., Luo, D., Si, Y., & Wang, B. (2024). Water Network-Augmented Two-State Model for
488 Protein-Ligand Binding Affinity Prediction. *Journal of chemical information and modeling*, 64(7), 2263–
489 2274. <https://doi.org/10.1021/acs.jcim.3c00567>

490 Schiebel, J., Gaspari, R., Wulsdorf, T., Ngo, K., Sohn, C., Schrader, T. E., et al. (2018). Intriguing role of
491 water in protein-ligand binding studied by neutron crystallography on trypsin complexes. *Nature*
492 *Communications*, 9(1), 3559. <https://doi.org/10.1038/s41467-018-05769-2>

493 Srinivasa, M., Gopal, S. M., Klumpers, F., Christian Herrmann, C., Lars V. Schäfer, L. V. (2017). Solvent
494 effects on ligand binding to a serine protease *Physical Chemistry Chemical Physics* 19, 10753-
495 10766 <https://doi.org/10.1039/C6CP07899K>

496 Sugahara, M., Takehira, M., & Yutani, K. (2013). Effect of heavy atoms on the thermal stability of α -
497 amylase from *Aspergillus oryzae*. *PLoS one*, 8(2), e57432. <https://doi.org/10.1371/journal.pone.0057432>

498 Timasheff, S. N. (2002). Protein-solvent preferential interactions, protein hydration, and the modulation of
499 biochemical reactions by solvent components. *Proceedings of the National Academy of Sciences of the*
500 *United States of America*, 99(15), 9721–9726. <https://doi.org/10.1073/pnas.122225399>

501 Tomasik, P. (2009). Specific chemical and physical properties of potato starch. *Food*, 9, 45–46

502 Udema, I. I. (2016) Determination of translational velocity of reaction mixture components: Effect on the
503 rate of reaction. *Advances in Biochemistry* 4 (6), 84-93. <https://doi.org/10.11648/j.ab.20160406.13>

504 Udema, I. I. & Onigbinde, A. O. (2019). Enzymatic kinetic issues and controversies surrounding Gibbs
505 free energy of activation and Arrhenius activation energy *Asian Journal of Physical and Chemical*
506 *Sciences* 7(4), 1-13 <https://doi.org/10.9734/AJOPACS/2019/v7i430103>

507 Udema, I. I. (2020). Effect of salts and organic osmolytes is due to conservative forces *Asian Journal of*
508 *Applied Chemistry Research* 5(1), 1-17, <https://doi.org/10.9734/AJACR/2020/v5i130123>

509 Udema, I. I. (2023). Directly and indirectly determinable rate constants in Michaelian enzyme-catalyzed
510 reactions *Asian Journal of Biochemistry, Genetics and Molecular Biology* 15 (1), 41-55,
511 <https://doi.org/10.9734/AJBGMB/2023/v15i1327>

512 Vonrhein, C., Schlauderer, G. J., & Schulz, G. E. (1995). Movie of the structural changes during a
513 catalytic cycle of nucleoside monophosphate kinases. *Structure (London, England: 1993)*, 3(5), 483–490.

514 Wade, R. C., Gabdouliline, R. R., Lüdemann, S. K., & Lounnas, V. (1998). Electrostatic steering and ionic
515 tethering in enzyme-ligand binding: Insights from simulations. *Proceedings of the National Academy of*
516 *Sciences of the United States of America*, 95(11), 5942–5949. <https://doi.org/10.1073/pnas.95.11.5942>

517 Yoshida N. (2017). Role of Solvation in Drug Design as Revealed by the Statistical Mechanics Integral
518 Equation Theory of Liquids. *Journal of Chemical Information and Modeling*, 57(11), 2646–2656.
519 <https://doi.org/10.1021/acs.jcim.7b00389>

520 Young, T., Abel, R., Kim, B., Berne, B. J., & Friesner, R. A. (2007). Motifs for molecular recognition
521 exploiting hydrophobic enclosure in protein-ligand binding. *Proceedings of the National Academy of*
522 *Sciences of the United States of America*, 104(3), 808–813. <https://doi.org/10.1073/pnas.0610202104>

523 Zsidó, B. Z., & Hetényi, C. (2021). The role of water in ligand binding *Current Opinion in Structural*
524 *Biology* 67, 1–8 <https://doi.org/10.1016/j.sbi.2020.08.002>

525
526